

Simulation of Direct Thrust Control for Linear Induction Motor Including End-Effect

M. Ali Usta

Dept. of Electrical and Electronics
Engineering, Karadeniz Technical
University, Trabzon/Turkey
mausta@ktu.edu.tr

Omur Akyazi

Sürmene Abdullah Kanca VHS,
Karadeniz Technical University,
Trabzon/Turkey
oakyazi@ktu.edu.tr

A. Sefa Akpinar

Dept. of Electrical and Electronics
Engineering, Karadeniz Technical
University, Trabzon/Turkey
akpinar@ktu.edu.tr

Abstract—In this paper, a direct thrust control (DTC) of linear induction motor (LIM) has been developed and a comprehensive study is presented. DTC is a method based on primer flux control in the stationary reference frame using direct control of the inverter switching. The basic concept of DTC is to control both primer flux and electromagnetic thrust of the machine simultaneously. Modeling phase begins with a derivation of suitable mathematical model to describe LIM in the stationary α - β reference frame. Then, the concept of DTC based on switching table (ST-DTC) strategy is illustrated and dealt with in detail. Finally, the performance of this control method has been demonstrated by simulations performed using Matlab/Simulink and the results obtained from the simulations are discussed.

Keywords—direct thrust control; switching table; vector control; linear induction motor; end effect.

I. INTRODUCTION

Linear electric motors (LEMs) belong to the group of special electrical machines. LEMs convert electrical energy directly into mechanical energy of linear motion. Thus, there is no need to wheel, gear or any type of mechanical rotary-to-linear converters. The most popular of LEMs are linear induction motors (LIMs). Nowadays, LIMs are widely used in transportation systems and in many industrial applications such as conveyor systems, elevators, actuators, material handling, hammers, presses, mills, separators, textile shuttles, sliding door, robots, etc [1-2]. But LIMs have some drawbacks due to its own structure of a finite core length. The most important problem is called “End Effects”. The end effects occur from the relative motion between primary and secondary. As the primary moves, it continuously encounter with a new secondary sheet. This new secondary sheet tends to resist a sudden increase in flux penetration and only permits a gradual accumulation of flux density in the air gap [3]. This influence on the flux density leads to braking force and additional loss that are produced by eddy currents at the entry and exit rail [4]. So, the end effects should be considered in both the modeling and controlling of LIMs in order to achieve speed or thrust tracking.

In recent years, direct thrust control (DTC) is preferable to give a fast and good dynamic thrust response in the small and medium power range applications. This control method is different in terms of the operation principle from the field oriented control (FOC) or the vector control technique. As the vector control is a method based on primer current control in the synchronous reference frame, DTC is a

method based on primer flux control in the stationary reference frame [5]. DTC has very simple control structure in comparison with the conventional vector control and is characterized by a good and fast dynamic response.

DTC-based drives do not require the coordinate transformation between stationary frame and synchronous frame and the inverter is directly controlled by the inverter switching states selected using switching table. Thus, neither current controllers nor pulse-width modulation (PWM) modulator is needed [6]. However this DTC approach has some disadvantages such as difficulty to control thrust and flux at very low speed, high current and thrust ripple, variable switching frequency due to the hysteresis comparators used for the thrust and flux comparators and high noise level at low speed [7].

The main objective of this paper is to develop the simulink model of direct thrust control of linear induction motor. The rest of the paper is organized as follows. Firstly, the mathematical model of linear induction motor in stationary reference frame is presented. Second, the principals of direct thrust control including end effects are introduced. Finally, the simulation results and some conclusions are given.

II. MODELING OF LINEAR INDUCTION MOTOR

To obtain a suitable LIM equivalent circuit, we must quantify the end effects during entry and exit from the secondary. So, the end effect is modeled by $f(Q)$ which is represented by:

$$f(Q) = \frac{1 - e^{-Q}}{Q} \quad (1)$$

Where, Q is a factor related to not only the primary length but also the machine velocity.

$$Q = \frac{DR_r}{L_r v} \quad (2)$$

It can be seen in (2) that the Q factor is inversely dependent on the velocity. i.e. for a zero velocity the end effects can be neglected ($Q=\infty$, $f(Q)=0$). As the velocity increases, the end effects increase and this causes a reduction of the magnetization current of LIM. This effect

may be quantified by modifying the magnetization inductance as follows.

$$L'_m = L_m(1 - f(Q)) \quad (3)$$

On the other hand, ohmic losses occurring with the increase of the eddy currents induced at the entry and exit ends of the secondary must be taken into consideration when the equivalent circuit is created. So, a resistance inserts in series with the inductance in the magnetization branch of the equivalent electrical circuit. This resistance represents the ohmic losses produced by the eddy currents and it is described as the product of the secondary resistance R_r by the $f(Q)$ factor.

$$R_{eddy} = R_r f(Q) \quad (4)$$

The equivalent circuit of the LIM is presented as shown in Fig. 1. This circuit is on a per phase basis.

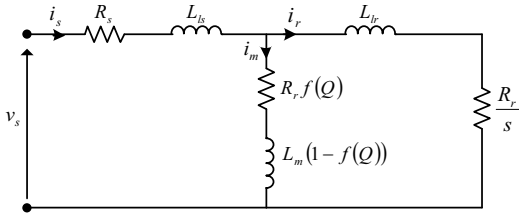


Figure 1. Per-phase LIM equivalent circuit

This equivalent model must be expressed in the synchronous reference frame (d-q model) or the stationary reference frame (α - β model) in order to develop the dynamic analysis and model-based control algorithms of LIM. In this study, the stationary reference frame is used to analyze the dynamic model including end effects of the LIM. Fig. 2 shows the α - β model of the equivalent circuit considering the end effects.

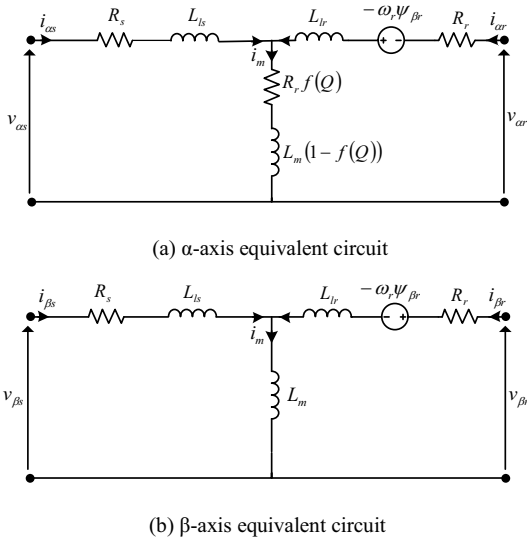


Figure 2. α - β equivalent circuit of the LIM with the end effects in the stationary frame

From the α - β equivalent circuit of LIM, the primary and secondary flux equations are given as follows.

$$\frac{d\psi_{cs}}{dt} = v_{cs} - R_s i_{cs} - R_r f(Q)(i_{cs} + i_{cr}) \quad (5)$$

$$\frac{d\psi_{\beta s}}{dt} = v_{\beta s} - R_s i_{\beta s} \quad (6)$$

$$\frac{d\psi_{cr}}{dt} = -R_r i_{cr} - R_r f(Q)(i_{cs} + i_{cr}) - \omega_r \psi_{\beta r} \quad (7)$$

$$\frac{d\psi_{\beta r}}{dt} = -R_r i_{\beta r} + \omega_r \psi_{cr} \quad (8)$$

The primary and secondary current equations are given as follows.

$$i_{cs} = \frac{(L_r - L_m f(Q))\psi_{cs} - L_m(1-f(Q))\psi_{cr}}{(L_s - L_m f(Q))(L_r - L_m f(Q)) - L_m^2(1-f(Q))^2} \quad (9)$$

$$i_{cr} = \frac{(L_s - L_m f(Q))\psi_{cr} - L_m(1-f(Q))\psi_{cs}}{(L_s - L_m f(Q))(L_r - L_m f(Q)) - L_m^2(1-f(Q))^2} \quad (10)$$

$$i_{\beta s} = \frac{L_r \psi_{\beta s} - L_m \psi_{\beta r}}{L_\sigma} \quad (11)$$

$$i_{\beta r} = \frac{L_s \psi_{\beta r} - L_m \psi_{\beta s}}{L_\sigma} \quad (12)$$

The thrust force and the motion equation are expressed as equation (13) and (14), respectively.

$$T_e = \frac{3}{2} \frac{\pi}{\tau_p} \frac{p}{2} (\psi_{cs} i_{\beta s} - \psi_{\beta s} i_{cs}) \quad (13)$$

$$T_e = m \frac{dv}{dt} + Bv + T_L \quad (14)$$

Where subscripts 's' and 'r' denote the primary and secondary values, respectively; subscripts ' α ' and ' β ' denote α -axis and β -axis values, respectively; p is the poles number; v is the linear primary speed in m/s; D is the primary length in meters; τ_p is the pole pitch; T_L is the load thrust force; B is the viscous friction coefficient of the LIM; m is the mass of the LIM.

III. DIRECT THRUST CONTROL

Fig. 3 shows the basic direct thrust control scheme which is similar to that for RIM.

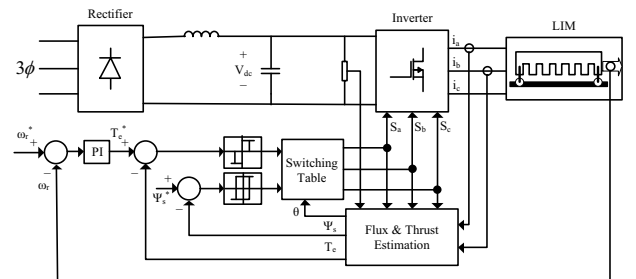


Figure 3. Basic direct thrust control scheme for linear induction motor

The basic principle of DTC is to control both primer flux and thrust directly by selecting the optimum inverter switching states [8]. As shown in Fig. 3, to determine the optimum voltage vector, the reference values (T_e^* and Ψ_s^*) are compared with the actual values calculated from primer

variables. The error signals obtained at the end of the comparison are applied to the three-level thrust and two-level flux hysteresis comparators. Then, the optimum voltage vector is selected by using the outputs of the

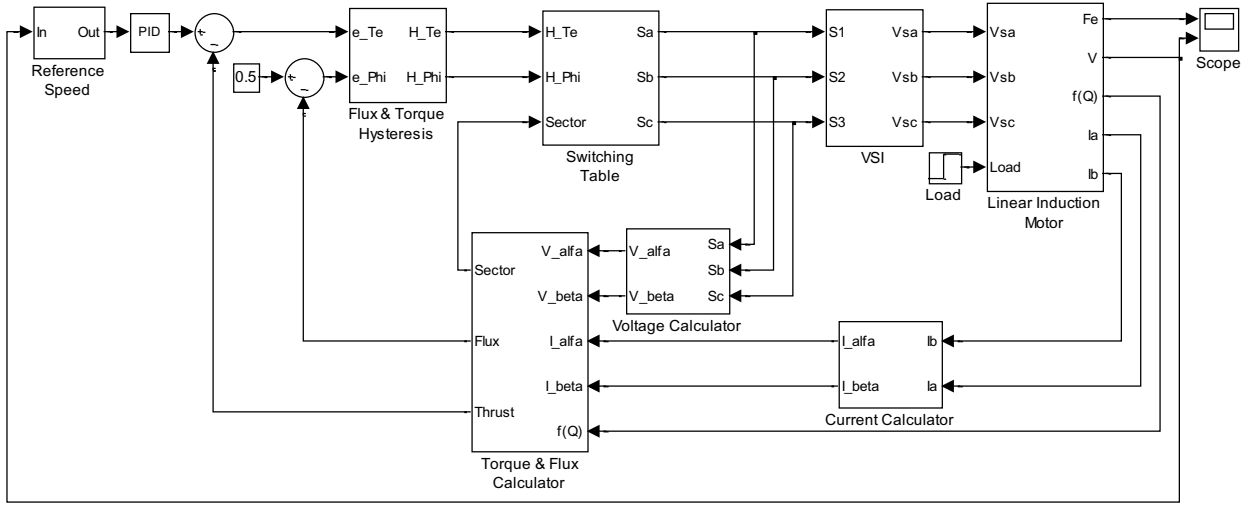


Figure 4. Simulink model of DTC for LIM with end effects

comparators and knowledge of the position of the primer flux at the switching table. This selection maintains the primer flux and thrust error inside their respective hysteresis bands. The switching table is shown in Table I. In the six-pulse VSI, there are six non-zero active voltage vectors and two zero voltage vectors. These are shown in Fig. 5.

TABLE I. SWITCHING TABLE

Flux error position	Thrust error position	Sector I	Sector II	Sector III	Sector IV	Sector V	Sector VI
1	1	V2	V3	V4	V5	V6	V1
	0	V7	V0	V7	V0	V7	V0
	-1	V6	V1	V2	V3	V4	V5
0	1	V3	V4	V5	V6	V1	V2
	0	V0	V7	V0	V7	V0	V7
	-1	V5	V6	V1	V2	V3	V4

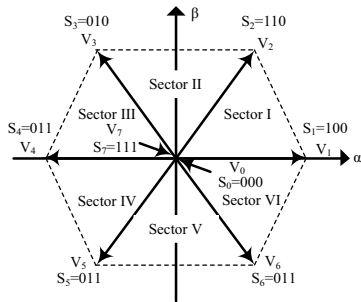


Figure 5. VSI voltage vectors

The actual values of the primer flux and thrust are obtained by using a closed-loop estimator and α - β components of primer voltage and primer current space vectors in the stationary reference frame are obtained from the state of switches of the inverter which is represented by S_A , S_B and S_C in Fig. 3. Primer voltage components ($V_{\alpha s}$, $V_{\beta s}$) are calculated as follows.

$$V_{\alpha s} = \frac{2}{3} V_{dc} \left(S_A - \frac{S_B + S_C}{2} \right) \quad (15)$$

$$V_{\beta s} = \frac{1}{\sqrt{3}} V_{dc} (S_A - S_C) \quad (16)$$

On the other hand, primer current components ($i_{\alpha s}$, $i_{\beta s}$) are calculated as follows.

$$i_{\alpha s} = i_{S_A} \quad (17)$$

$$i_{\beta s} = \frac{i_{S_A} + 2i_{S_B}}{\sqrt{3}} \quad (18)$$

It is important to determine accurately the knowledge of the primer flux and thrust for DTC. So, the end effects are considered while the primer flux and thrust are estimated. In this case, the primer flux is derived from (5) and (6).

$$\psi_{\alpha s} = \int (v_{\alpha s} - R_s i_{\alpha s} - R_r f(Q) i_{\alpha s}) dt \quad (19)$$

$$\psi_{\beta s} = \int (v_{\beta s} - R_s i_{\beta s}) dt \quad (20)$$

$$|\psi_s| = \sqrt{\psi_{\alpha s}^2 + \psi_{\beta s}^2} \quad (21)$$

In equation (5), α -axis secondary current is ignored due to its measurement difficulty and less effect on the flux estimation [9]. The position of primer flux is denoted by θ_ψ and given by equation (22).

$$\theta_\psi = \tan^{-1}\left(\frac{\psi_{\beta s}}{\psi_{\alpha s}}\right) \quad (22)$$

The thrust value is estimated as follows.

$$T_e = \frac{3}{2} \frac{\pi}{\tau_p} \frac{p}{2} (\psi_{\alpha s} i_{\beta s} - \psi_{\beta s} i_{\alpha s}) \quad (23)$$

IV. SIMULATION RESULTS

Simulink model of DTC-based drive system for LIM considering the end effects is shown in Fig. 4. In this part, the validity of the control system is examined under different conditions. A step change of thrust command is applied at the beginning of the simulation from 0 to 10 Nm and this command is not changed until the end of the simulation. The primer flux reference is set to 0.5 Wb. During the simulation, the different reference speed is applied to the system. Firstly, the system is sped up with the acceleration of 10 m/s^2 until from 0 to 0.3 second. Secondly, a constant speed that is 3 m/s is applied to the system between 0.3 to 0.7 second and finally the system is decelerated with the acceleration of 10 m/s^2 between 0.7 to 1 second. Fig.6, Fig. 7 and Fig. 8 show the speed, thrust and flux linkage trajectory responses, respectively. Fig. 9 and Fig. 10 show the estimated primer flux and thrust, respectively.

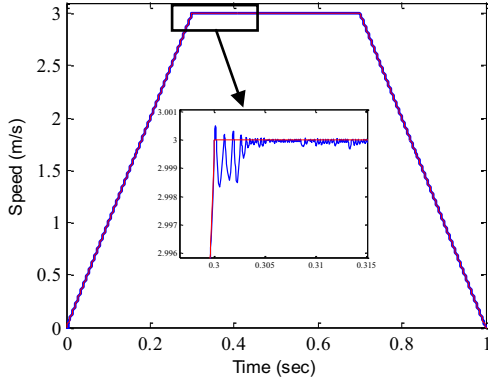


Figure 6. The speed response of LIM with DTC-based drive

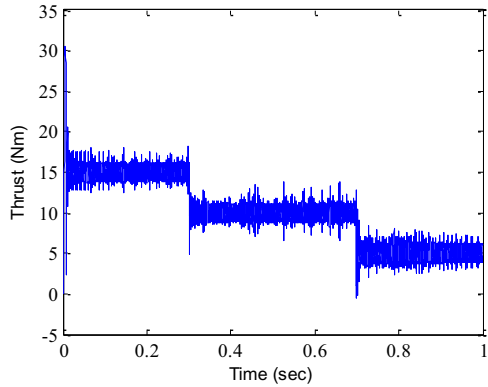


Figure 7. The thrust response of LIM with DTC-based drive

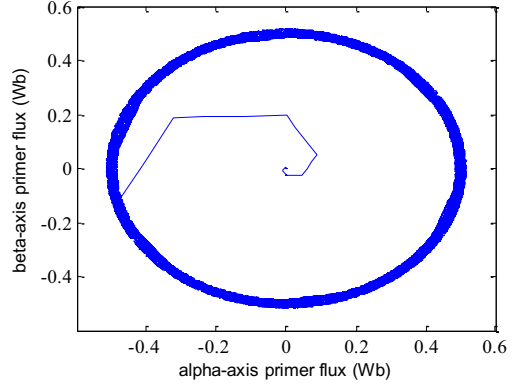


Figure 8. The primer flux trajectory of LIM with DTC-based drive

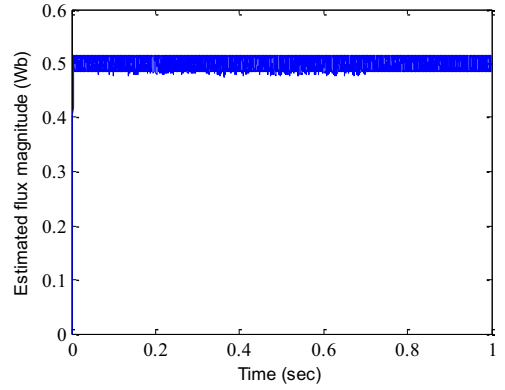


Figure 9. Estimated primer flux magnitude waveform

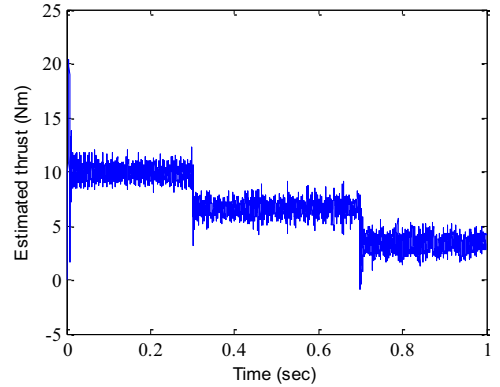


Figure 10. Estimated thrust waveform

V. CONCLUSION

This paper presents a dynamic model and a DTC-based drive system for LIM including end effects and it is focused to develop a direct thrust control simulink model. A classical DTC is used, but unlike a conventional DTC used for RIM, the flux and thrust equations are improved considering the end effects and these equations are used at the flux and thrust estimator. The given improvement is validated by the simulation results. It can be seen from simulation results that the proposed method has been given fast thrust and speed response and this method can be preferable for the small and medium power range applications.

APPENDIX

The test machine has the following parameters as shown in Table II.

TABLE II. PARAMETERS OF TESTED LINEAR INDUCTION MACHINE [9]

Number of Poles–P	2
Primary Resistance–Rs	2.82 Ω
Secondary Resistance–Rr	48.84 Ω
Primary Inductance–Ls	0.0452 H
Secondary Inductance–Lr	0.0301 H
Magnetizing Inductance–Lm	0.0262 H
Pole Pitch– τ_p	0.06 m
Primary Length–D	0.21 m

REFERENCES

- [1] Jacek F. Gieras, "Linear Induction Drives", Clarendon Press, Oxford, 1994.
- [2] A. Boucheta, I. K. Bousserhane, A. Hazzab, B. Mazari and M. K. Fellah, "Linear Induction Motor Control Using Sliding Mode Considering the End Effects", 6th International Multi-Conference on Systems, Signals and Devices, March 23-26, 2009, Djerba, Tunisia.
- [3] J. Duncan, "Linear Induction Motor – Equivalent Circuit Model", in IEE Proc., Vol. 130, pp. 51-57, January, 1983.
- [4] A. Z. Bazghaleh, M. R. Naghashan, H. Mahmoudimanesh and M. R. Meshkatoddini, "Effective Design Parameters on the End Effect in Single-Sided Linear Induction Motors", World Academy of Science, Engineering and Technology, pp. 95-100, April, 2010.
- [5] H. F. A. Wahab and H. Sanusi, "Simulink Model of Direct Torque Control of Induction Machine", American Journal of Applied Sciences, Vol. 5, pp. 1083-1090, August, 2008.
- [6] Y. S. Lai and J. H. Chen, "A New Approach to Direct Torque Control of Induction Motor Drives for Constant Inverter Switching Frequency and Torque Ripple Reduction", IEEE Transactions on Energy Conversion, Vol. 16, No. 3, pp. 220-227, September, 2001.
- [7] D. Casadei, F. Profumo, G. Serra and A. Tani, "FOC and DTC: Two Viable Schemes for Induction Motors Torque Control", IEEE Transactions on Power Electronics, Vol. 17, No. 5, pp. 779-787 September, 2002.
- [8] V. D. Colli, F. Marignetti, M. Scarano and M. M. Radulescu, "Implementation of an Improved Direct Thrust and Flux Control for Linear Induction Motors", Electric Machines and Drives Conference, Vol. 1, pp. 488-493, 1-4 June, 2003.
- [9] B. Susluoglu and V. M. Karshi, "Direct Thrust Controlled Linear Induction Motor Including End Effect", Power Electronics and Motion Control Conference, pp. 850-854, 1-3 September, 2008.
- [10] E. Ozkop, A. S. Akpınar and H. I. Okumus, "Direct Torque Control for Linear Induction Motor", 12th International Middle-East Power System Conference, pp. 373-376, 12-15 March, 2008.
- [11] E. Ozkop and H. I. Okumus, "Direct Torque Control of Induction Motor Using Space Vector Modulation (SVM-DTC)", 12th International Middle-East Power System Conference, pp. 368-372, 12-15 March, 2008.
- [12] B. Kwon, K. Woo and S. Kim, "Finite Element Analysis of Direct Thrust-Controlled Linear Induction Motor", IEEE Transactions on Magnetics, pp. 1306-1309, May 1999.
- [13] K. Itoh and H. Kubota, "Thrust Ripple Reduction of Linear Induction Motor with Direct Torque Control", Proceedings of the 8th International Conference on Electrical Machines and Systems, Vol. 1, pp. 655-658, 27-29 September, 2005.
- [14] S. Meziane, R. Toufouti and H. Benalla, "Review of Direct Torque and Flux Control Methods for Voltage Source Inverter Fed Induction Motor", Journal of Automatic Control and System Engineering, Vol. 6, pp.47-53, October, 2006.